The sea is your mirror

Marc Parenthoen, Fred Murie, Flavien Thery

The Sea Is Your Mirror

Marc Parenthoen[1]*, Fred Murie[2]† and Flavien Thery[2]‡
(1) Lab-STICC, ENIB, UEB (2) SPECULAIRE, SIANA

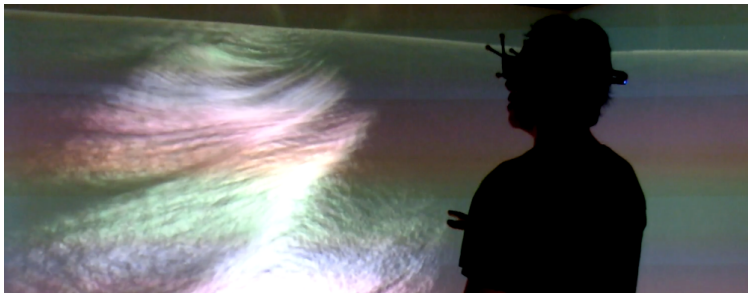

Figure 1: *Feel like Poseidon's apprentice.*

Abstract

The Sea Is Your Mirror is an artistic interactive experience where surface cerebral electromagnetic waves from a participant wearing an EEG sensor headset are depicted in real-time as ocean waves in an animated 3D environment. The aim of this article is to describe the sea wave model used for the sea state animation and how it is connected to the brain computer interface (BCI). The sea state is animated by the *groupy choppy wave model* that provides nonlinear sea states with wave groups and asymmetric wave shapes. The BCI maps the temporal spectrum of the electroencephalogram onto the elevation spectrum of the sea surface. The resulting setup enables the participant to fly over a dynamic sea state: a metaphor for conscious and unconscious neurofeedback.

CR Categories: I.3.7 [Computer Graphics]: Three-Dimensional Graphics and Realism—Animation; I.3.7 [Computer Graphics]: Three-Dimensional Graphics and Realism—Virtual reality;

Keywords: sea wave, EEG, BCI, natural phenomena, animation, virtual reality, art and science

1 Introduction

The Sea Is Your Mirror is an artistic interactive experience, which enables users to project their minds onto a virtual ocean projected onto a wall in an exhibition space. Equipped with an electroencephalogram (EEG) sensor headset, participants watch their brain activity being converted into ocean movements. Users therefore come face-to-face with an intimate panorama, ruled by their own inner life. He may seek to control it or merely to contemplate the seascape. Any brain activity measured on the EEG instantly produces effects on the projected image, which can therefore be seen in real-time. In this way, subjects of the experience are immersed in a feedback loop generated by each of their thoughts. They share an allegorical image of his mind with other viewers within the exhibition space. The depths of the users' minds nonetheless remain unfathomable.

The use of an EEG interface is relatively new in art and science projects. It has been used to control the movement of a steel door in *Suspension of Attention* [Chatonsky 2013], to illustrate a metaphor of an artist's emotional state in *Eunoia* [Park 2013] or to learn meditation through neurofeeedback in *LIAison-EEG:EGG* [Min 2013]. In *The Sea Is Your Mirror*, the EEG allows users to fly over an animated ocean, which is a metaphor of the their own mind.

To obtain such an artistic operational setup, we required some contributions from virtual reality. The scientific challenges we examine in this paper are:

1. firstly a Brain Computer Interface (BCI) question:
   how can the EEG be connected to virtual sea state parameters in a reliable way which also increases users' feeling of influence?

2. and secondly an animation question:
   how can choppy but believable ocean waves be animated in real-time?

As far as we know, this is the first study in which an EEG has been converted into sea waves. Here the BCI attaches the wavelength of each ocean wave to an EEG area at a given frequency range. Wave heights are calculated by averaging the energy emmitted by given areas and frequency ranges over time windows that are proportional to the attributed sea wave periods. In addition to sea surface animation, the color of the moonlight is controlled using simple EEG-based emotion recognition. The ability to turn (left/right) while in flight is controlled by mere thought. We will discuss the suitability of the process to participative experiments and its robustness from the point of view of multiple users.

With regards to the animation of ocean waves; since the pioneering works of the eighties, graphic primitives used for large ocean scenes have been the sinusoidal map [Mastin et al. 1987] or its choppy equivalent: the hypo-cycloidal map [Fournier and Reeves 1986; Peachey 1986]. In this contribution, we adapt a lesser-known model based on a reified 2D Morlet wavelet as a graphic primitive for ocean wave animation [Parenthoen et al. 2004]. These early

*marc.parenthoen@enib.fr, http://www.cerv.org
†fredmurie@stationgraphique.com, http://www.speculaire.fr
‡flavien.thery@free.fr, http://www.siana.eu

works directly represent wave groups[1]. We equip them with a relevant novel instant phase model to capture usual vertical choppy asymmetries as well as horizontal asymmetries. In such a group model, energy distribution is not necessarily uniform, which can lead to very different wave structures having the same spectra. Furthermore, horizontal and vertical displacements are organized so that self-intersection no longer seems to be a crucial problem, even for very stormy conditions.

2 Related Work

2.1 EEG: a BCI for Control and Emotion

Because EEG is a non-invasive sensor, the rise of brain computer interface (BCI) studies [Birbaumer 2006] makes EEG sensor headsets a center of interest for experiments in virtual reality [Lécuyer et al. 2008]. As BCIs initially aimed to reflect conscious neurophysiological processes, their main use has been conscious control of virtual words through a learning process. OpenVibe is an example of a development suite which experiments with this goal [Renard et al. 2010].

Even if the range of EEG energy is very wide (from less than 0.05Hz to more than 100Hz) only frequencies from 0.5Hz to 40Hz are common, and they are partitioned into five classes: $\delta \in [0.5, 4[$, $\theta \in [4, 8[$, $\alpha \in [8, 13[$, $\beta \in [13, 20[$ and $\gamma \in [20, 40[$. Put simply, these classes can relate to cognitive states: δ for deeper sleep, θ for light sleep and meditation, α for conscious dreaming, β for conscious cognition and γ for active reasoning. These frequency limitations (0.5Hz to 40Hz) are mainly due to artifacts, which make it difficult to separate cerebral activity from other causes, such as muscular activity or electrode movement, into categories of EEG signals. Automatic artifact detection, even in the 0.5Hz to 40Hz range, remains a challenge [Fatourechi et al. 2007]. In real-time this causes particular difficulty, and needs to be done for BCI: this may explain why 25% of people cannot calibrate a BCI [Vidaurre and Blankertz 2010].

These previous EEG as BCI studies nonetheless show that it is quite easy to distinguish between thinking about left movements and thinking about right movements, simply by analyzing changes in β and γ range energy in the premotor cortex (frontal lobes). An increase in activity on the right means thoughts about movement on the left, while an increase in activity on the left means thoughts about movement on the right. This will be used in *The Sea Is Your Mirror* to turn left or right during the flight over the virtual sea.

The other use of the EEG is to recognize users' emotions [Jones and Fox 1992]. For EEG-based emotion recognition in games see the review by Bos et al. [2010]. All the available methods require training periods and are very sensitive to artifacts. One thing that seems to unify 20 years of experiments is that some valence distinction in positive/negative emotions is correlated with the evolution of the α and β range energy upon the preforontal cortex: an increase on the left means positive, while an increase on the right means negative emotion. We will use this to adjust the color of the moonlight in *The Sea Is Your Mirror*.

2.2 Sea State Animation

Both of the existing graphic primitives are solutions of linear approximations of the so-called Navier-Stokes equations governing ocean surface waves, in Eulerian coordinates for the sinusoidal map (Airy wave theory), or in Lagrangian coordinates for the hypocycloidal map (Gerstner's swell).

Tessendorf proposed a Fourier-based method which respects an oceanographic elevation spectrum with discretization for wave propagation speed according to the wavelength that is relevant for repeating dynamic ocean motifs [Tessendorf 2001]. The visualization grid has been adapted to the camera's perspective in order to decrease computing complexity when flying over the ocean [Hinsinger et al. 2002]. Over the next decade these Fourier-based methods, enriched by horizontal movements, were used in cinematographic productions. Some isolated breaking waves have been added by using numerical schemes from computational fluid dynamics (CFD) [Darles et al. 2011], but the current choppy models for large-scale sea scenes which are based on first-order primitives only provide vertical asymmetries[2] and need significant computations for solving self-intersections [Nielsen et al. 2013]. Furthermore, the explicit notion of "wave group" is lacking in most current models.

However, oceanographers agree that nonlinear effects in the Navier-Stokes equations make waves organize themselves into groups [Meyers et al. 1993; Liu et al. 1995; Donelan and Drennan 1996] and express horizontal asymmetries [Stansell et al. 2003]. Despite considerable progress in CFD, simulating a sea surface of several square kilometers with wave groups and asymmetric waves in real-time remains impossible [Nielsen and Bridson 2011]. In addition, dealing with boundary conditions during such free exploration over the virtual ocean would be difficult.

Related works have therefore shown that this seems to be the first time an EEG has been connected to a virtual sea scene and that real-time animation of stormy sea state remains a challenging task.

3 Connecting the EEG to the Sea Scene

In this section, we explain how we connected the EEG to the virtual environment. First, we will describe the general features of how we calculated cerebral activity values from the raw data from the headset. These cerebral activity indicators will then be converted according to three objectives: wave height, flight direction and moonlight color.

3.1 From EEG to Cerebral Activity Indicators

From each EEG electrode, we sampled the last second of the signal at $128\,Hz$, and computed electrical energy at every frequency between $4\,Hz$ and $40\,Hz$ thanks to a Discrete Fourier Transform. Data was not filtered in advance, but when an electrode was not operational (not grounded), its data value was set to zero.

By summing the square moduli of the previous Fourier coefficients over frequencies lying respectively in θ, α, β, and low, medium and high γ ranges, we obtained six respective values that were proportional to the corresponding electrical energy for each electrode at every frequency range. Then we simply added the energies of the electrodes in a given area in order to obtain the value indicating surface electrical brain activity in the given area at a given frequency range.

[1] In oceanography [Komen et al. 1994], wave groups are distinct from wave trains: a wave group is an empirical phenomenon, while a wave train is a theoretical mathematical object.

[2] In oceanography [Stansell et al. 2003], wave asymmetries are defined using 4 times: T_1 from crest to down zero-crossing, T_2 from down zero-crossing to trough, T_3 from trough to up zero-crossing and T_4 from up zero-crossing to crest. Vertical symmetry occurs when $T_2 + T_3 = T_1 + T_4$, that is to say that time below zero equals time above zero. Horizontal symmetry occurs when $T_1 + T_2 = T_3 + T_4$, that is to say that downward time equals upward time.

For *The Sea Is Your Mirror* at Siana [Catala 2015], we used 4 areas on the scalp: front left, front right, back left and back right. This gave $4_{areas} \times 6_{freq.\,ranges} = 24$ indicators. These 24 indicators were calculated and sent to the animation process at approximately $10\,Hz$. It must be noted that if none of the electrodes corresponding to a given area are operational for more than one second, then the 6 corresponding indicators are null.

These indicators are very spiky, so average values needed to be used. A less complex way of averaging in real-time with the variable time-step δt is to estimate the mean by exponential forgetting with a life time τ:

$$\bar{v}_{(t)} = \alpha v_{(t)} + (1-\alpha)\bar{v}_{(t-\delta t)}, \text{ with } : \alpha = min(1, \delta t/\tau) \quad (1)$$

where δt is the time elapsed since the last calculation of the average, and α is the forgetting coefficient. In order to understand the life time τ, if the v value becomes a constant v_0, time τ allows the approximated average $\bar{v}$ to nearly reach the target v_0 in $\sim \tau/\delta t$ steps.

3.2 From Cerebral Indicators to Sea Scene

Cerebral activity indicators are converted for three objectives: flight direction, moonlight color, and wave height.

3.2.1 EEG Controls Flight Direction

In order to control flight direction, the state-of-the-art method requires two areas situated to the right and to the left of the premotor cortex, and to use β and γ left-right differences. Let $\mathcal{T}_{right}$ be the logarithm for the sum of β and γ activity indicators over the right premotor area, and $\mathcal{T}_{left}$ the left equivalent.

What is important is not absolute difference, but relative difference: that is to say the difference relative to average activity. In order to calculate this, we use equation (1) applied twice to $\mathcal{T}_{right}$ and twice to $\mathcal{T}_{left}$ with two different life times $\tau_{fast} = 1\,s$ and $\tau_{slow} = 10\,s$:

$$\overline{\mathcal{T}^{fast}_{right}}(t) = \alpha_{fast}\mathcal{T}_{right}(t) + (1-\alpha_{fast})\overline{\mathcal{T}^{fast}_{right}}(t-\delta t) \quad (2)$$

$$\overline{\mathcal{T}^{fast}_{left}}(t) = \alpha_{fast}\mathcal{T}_{left}(t) + (1-\alpha_{fast})\overline{\mathcal{T}^{fast}_{left}}(t-\delta t) \quad (3)$$

$$\overline{\mathcal{T}^{slow}_{right}}(t) = \alpha_{slow}\mathcal{T}_{right}(t) + (1-\alpha_{slow})\overline{\mathcal{T}^{slow}_{right}}(t-\delta t) \quad (4)$$

$$\overline{\mathcal{T}^{slow}_{left}}(t) = \alpha_{slow}\mathcal{T}_{left}(t) + (1-\alpha_{slow})\overline{\mathcal{T}^{slow}_{left}}(t-\delta t) \quad (5)$$

Then we compute right fast divided by right slow:

$$\mathcal{R} = \overline{\mathcal{T}^{fast}_{right}}(t)/\overline{\mathcal{T}^{slow}_{right}}(t) \quad (6)$$

and left fast divided by left slow:

$$\mathcal{L} = \overline{\mathcal{T}^{fast}_{left}}(t)/\overline{\mathcal{T}^{slow}_{left}}(t) \quad (7)$$

Turning is controlled by the following algorithm:

`if` $\mathcal{R} > 1$ *and* $\mathcal{R}/\mathcal{L} > 1$:
  turn left at a speed proportional to $\mathcal{R}/\mathcal{L} - 1$
`if` $\mathcal{L} > 1$ *and* $\mathcal{R}/\mathcal{L} < 1$:
  turn right at a speed proportional to $\mathcal{L}/\mathcal{R} - 1$
`default` :
  slowly reach predefined direction target

Rotation speed is also confined by extremum values and averaged by using equation (1) with a life time $\tau = 2\,s$, in order to avoid oscillations.

Furthermore, the feeling of flying over the ocean like an albatross depends on the behavior of the 3D viewer rendering the scene. Our viewer used a controller to maintain altitude above the sea surface. This controller was equipped with 7 perception points: 2 frontward, 2×2 sideward (each side) and one downward, in order to measure the sea height and automatically adapt altitude according to wave peaks and target altitude.

3.2.2 EEG Recognition of Mood Valence

In order to evoke mood, in accordance with related works, the color of the moonlight was adjusted depending on the emotion valence based on left/right average differences at α and β frequencies in the prefrontal cortex.

Let $\mathcal{M}_{right}$ be the logarithm of the sum of α and β activity indicators over the right prefrontal area. Compute $\overline{\mathcal{M}_{right}}$ and its left counterpart using formula (1), with life time $\tau = 30\,s$ as mood changes are supposed to be more gradual than changes in direction.

To determine changes in mood, we computed the left-right difference:

$$\mathcal{D} = \overline{\mathcal{M}_{right}}(t) - \overline{\mathcal{M}_{left}}(t)$$

We updated min and max values for $\mathcal{D}$ over the duration 2τ. The moonlight obeys the following formulas:

$$m = \frac{\mathcal{D} - \mathcal{D}_{min}}{\mathcal{D}_{max} - \mathcal{D}_{min}} \quad (8)$$

$$light_{color} = m \times neg_{color} + (1-m) \times pos_{color} \quad (9)$$

where $m \in [0, 1]$ because it is computed after min and max updates, neg_{color} is the color chosen by artists for drawing negative mood ($m = 1$) and pos_{color} is the color chosen by artists for drawing positive mood ($m = 0$).

3.2.3 EEG Connection to Wave Height

From a poetic perspective, the main idea was to translate the story of the users' brain activity (EEG) into an ocean wave story, as a metaphor for conscious activity. From a distant sleepy long swell to an iridescent sea wind due to a local storm, we translated temporal spectra of cerebral activity potentials into spatial spectra of sea wave elevations, while retaining the topology of wavelength maps. In other words, slow cerebral waves (sleep and meditation) should be represented by long sea waves (swell), while fast cerebral waves (active cognition and reasoning) should be represented by short sea waves (sea breeze and ripples).

We manually associated one brain activity indicator extracted from the EEG with one sea state wave vector. During the experiment at Siana [Catala 2015], we used 8 components for gravity waves with wavelengths ranging from one meter to one hundred meters, and 3 components for capillary waves, ranging from one centimeter to twenty centimeters.

Once an association between the pair (frequency range, area)$_{EEG}$ and the pair (wavelength, direction)$_{sea}$ is chosen, the sea wave height will result from a transformation of EEG energy e on the logarithm. This transformation uses the standard deviation σ of e and the average estimation $\bar{e}$ of e in accordance with equation (1) with a life time $\tau = 30\,s$. The target sea wave amplitude a_{target} is given by:

$$a_{target} = a_{max} \times f_c\left(\frac{e - \bar{e}}{\sigma}\right) \quad (10)$$

where a_{max} is the maximum amplitude determined by the artist for that wave vector, and where f_c is linear from $[-c, c]$ to $[0, 1]$, is null before $-c$ and has a value of one after c. We set $c = 2$, so that only 5% of e values could saturate f. $\tau = 30\,s$ was chosen to estimate averages and standard deviation because each user only plays for a

few minutes and the system must react as soon as possible after the game begins. If we use a_{target} for actual wave height immediately, the sea state animation looks chaotic and unrealistic as the wave heights change too quicky.

Once again, we used formula 1 to average a_{target} into actual wave amplitude a. To set τ values that increase the users' impression of influence on the sea state, we quickly experimented with nine users' τ values from one tenth of a second to one minute. These values were randomly selected in $\{0.1, 0.5, 1, 2, 5, 10, 20, 30, 45, 60\}$ seconds, and the whole EEG was used (full scalp and every range). A 2-minute animation was created for a single sinusoidal wave with $10\,m$ wavelength, $1\,m$ maximum height and $3\,s$ period. Subjects were asked: *"Do you have the impression that your thoughts are influencing the waves?"*. The result, which remains to be confirmed, is that τ values below 2 seconds give unrealistic dynamics for sea swells with no sensation of influence, and values above 30 seconds make the perception of influence disappear.

To keep the wind as a metaphor for conscious cerebral activity, we decided to set τ values proportional to sea wave periods; more precisely, artists chose the sea wave period for each τ value twice.

We have explained how the EEG can control flight direction, illustrate users' mood and offer dynamic amplitude values for connected sea wave vectors. These dynamic sea wave heights could be mapped to any sea model animated in real-time. We shall now explore the reflection of the sea in our metaphorical mirror.

4 Choppy Groupy Wave Model

In this section, we describe the model used for sea state animation. It stems from the groupy wave model in which the sea state results from the sum of interacting wave groups [Parenthoen et al. 2004]. A dynamic instant phase equips each wave group in order to enable vertical and horizontal asymmetries in an original choppy fashion.

4.1 Groupy Wave Model

Our graphic primitive is a wave group model that stems from ten years of interdisciplinary research. This wave group model is a good approximation for deep water solitons[3]. One single group acts on sea surface elevation $z(\vec{x}, t)$ as follows:

$$z(\vec{x}, t) = \zeta(\vec{x}, t) \cdot \sin\big(\phi(\vec{x}, t)\big) \tag{11}$$

where ζ is the group envelope and ϕ its phase, that obeys:

$$\phi(\vec{x}, t) = \vec{k}.(\vec{x} - \vec{x}_0) + \theta_0 - \omega t \tag{12}$$

where $\vec{x}_0$ is the group center position at $t = 0$, θ_0 is the phase at group center at $t = 0$, and $\vec{k}$ is its mean wave vector (k being its wave number). Its pulsation ω also follows the open sea dispersion relation:

$$\omega^2 = gk\left(1 + (k/k_m)^2\right) \tag{13}$$

where $k_m = \sqrt{\rho_w g/T} \approx 370 rad.m^{-1}$. While the ζ envelope is a Gaussian lens which is attached to the group center $\vec{x}_c$:

$$\zeta(\vec{x}, t) = a \cdot e^{\left(\frac{-(\vec{x} - \vec{x}_c(t))^2}{2\varrho^2}\right)} \tag{14}$$

[3]Water wave envelopes follow a nonlinear Hamiltonian equation [Zakharov 1968]. In deep water, envelope solitons may occur and our wave group model is an adequate approximation of such solitons, even if it is no longer a solution for the Navier-Stokes's equation linearization.

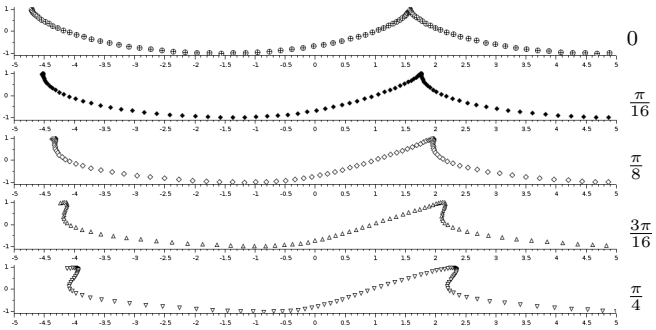

Wave shapes (without envelope) for different maximum crest advance values ϕ_{max} in our choppy model. All waves have the same steepness ($\zeta \cdot k = 1$). From the classical choppy model $\phi_{max} = 0$ with cycloidal shape and no horizontal asymmetry (top) to a crest advance reaching $\phi_{max} = \pi/4$ with a large horizontal asymmetry (bottom).

Figure 2: *Horizontal asymmetry as a function of crest advance*

with its envelope extension ϱ, its maximum amplitude a at its center $\vec{x}_c$ moving at group speed in open sea from $\vec{x}_0$ at $t = 0$:

$$\vec{x}_c = \vec{x}_0 + t \cdot \frac{\vec{c}}{2} \quad \text{and} \quad \varrho = n_{waves}\frac{\pi}{k} \tag{15}$$

where $\vec{c} = \omega\vec{k}/k^2$, is its phase speed. The envelope extension ϱ of the group is chosen greater than the wavelength $2\pi/k$ and is proportional to the number of waves $n_{waves} \geq 2$ actually expressed by the group.

We assume that the sea surface can be described by superimposing such wave groups linearly[4] when several groups act, the resulting elevation is the sum of elevations due to each group.

4.2 Choppy Instant Phases

Vertical asymmetries are well represented by classical choppy models: simply take equation 11 and use circular orbits instead of vertical movements. The result would be choppy wave groups with significant vertical asymmetries near the center, but no horizontal asymmetry would be observed. We then rewrite equation 11 in the $(\vec{k}, \vec{z})$ vertical plane with horizontal movements and instant phase:

$$\begin{cases} u = \zeta \cdot \cos(\phi + \delta\phi) \\ z = \zeta \cdot \sin(\phi) \end{cases} \tag{16}$$

where u is the horizontal displacement following $\vec{k}$ direction, z is the vertical displacement, and ζ is the local wave amplitude at position $\vec{x}$ and time t, with its phase ϕ and instant phase $\delta\phi$ as follows:

$$\begin{cases} \phi = \vec{k}.\vec{x} + \theta - \omega t \\ \delta\phi = \zeta \cdot k \cdot \phi_{max} \cdot p(\phi) \\ p(\phi) = \frac{(1-\sin\phi)^2}{2} - 1 \end{cases} \tag{17}$$

where the p function is smooth with image values in $[-1, 1]$, larger flats around -1 (near crests: $\phi \equiv \pi/2 \bmod 2\pi$) and smaller peaks around 1 (near troughs: $\phi \equiv -\pi/2 \bmod 2\pi$). The amount of horizontal asymmetry can be characterized by crest advance and trough delay, that we suppose both equal to ϕ_{max}. Instant phase $\delta\phi$ is proportional to local steepness ($\zeta \cdot k$) in order to increase horizontal

[4]Non-linear aspects of the complete groupy model come from interactions between wave groups and other modelized phenomena.

asymmetry only when non-linearity rises. In real sea states, maximum crest advance rarely exceeds $\pi/6$ radians. The larger the crest advance, the higher the horizontal asymmetry (Fig. 2). By increasing the crest advance rate of a group, an artist can create a highly non-linear wave and even an overhang without self-intersection and whose behavior will remain consistent with further animation.

It should be noted that the choppy version of the groupy wave model has fully-differentiable expressions thanks to equations (16) and (17). If analytical slopes, normals or speeds are required, simply express partial derivatives of u and z along $\vec{k}$ for geometric variables, and along t for water particle speed. Envelope ζ variations can be neglected as the envelope should evolve slowly according to wave dynamics. These expressions can be either inside the fluid (a full 3D field) where ζ depends also on altitude z, for example like a decreasing exponential function. It would therefore be possible to connect this model to spray generators or boat animations.

4.3 Wave group maps and textures

In order to populate the ocean by wave groups, we organized groups with the same mean wave vector $\vec{k}$ into group map, drawing on Belemaalem et al. [2010]. For rendering gust effects and ripples, the sea surface was also textured with normal mapping in proportion to γ-EEG activity.

4.3.1 Wave Group Maps

The EEG connection to wave heights gives an amplitude a for each attached wave vector. For a given wave vector $\vec{k}$, our map is the sum of wave groups which all have this wave vector $\vec{k}$. Each wave group in the map has its own maximum amplitude a_n in accordance with a Rayleigh distribution with parameter equal to the EEG given height a and its own phase θ_n uniformly distributed in $[0, 2\pi[$. Its own position center $\vec{x}_n$ is regularly distributed[5], so that the center positions $\vec{x}_n$ of groups occupy fixed positions relative to each other at vertices of a regular square grid travelling at group speed. Grid step size equals $2\varrho \times \max(1/2, 1/\sqrt{\lambda})$, where ϱ is the group envelope extension. The smaller λ, the greater the grid step. We chose this grid step size because when a point is more than 2ϱ from the center, the group influence becomes negligible and then can disappear from the sum. The parameter $\lambda, 0 < \lambda \leq 4$, can be interpreted as group density.

With this hypothesis, groups are identified by integer indices on the group map grid, and for a given map, the number of wave groups actually acting at any position is at most four (Fig. 3).

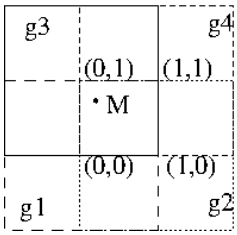

Finding indexes of the 4 groups acting on M is simply written as integer quotients of their coordinates relative to the referent group center by the grid step size, followed by 4 neighboring explorations at [+0,+0], [+0,+1], [+1,+0] and [+1,+1]. From the 4 pairs (i, j) resulting from the previous quotients and exploration, one can compute unique indices $i + p \times j$ that can follow groups and be used as a seed for computing random numbers a_n and θ_n attached to each group.

Figure 3: *Finding indexes of groups acting at a given point*

We used Unity3D[6] in order to enable artists to interact easily with the project, including its vertex and shader programs. We thus implemented in GLSL this algorithm for wave group maps.

4.3.2 High Frequency Normal Mapping with EEG γ Activity

The sea surface was also textured with normal mapping. In order to convert three different γ-EEG activities, the same texture was scaled and rotated three ways, then translated at the phase speed computed according to the scale and rotation applied. The peak wave number k of the normal bump texture at scale one was determined manually, and the phase speeds $v_i = \omega_i/k_i$ were computed thanks to the dispersion relation (13).

The bump normal is the weighted sum of these three transformed normal map textures, and the weighting coefficients are the cerebral activity indicators of low, medium, and high γ-EGG on the full scalp respectively.

The resulting normal is the average of the wave groups' geometric normals and the bump normals. This average is weighted to increase the bump normals when the total γ activity indicator is high. As a result of these calculations, when the users experience intense active reasoning, they see the effects of gusts on the sea surface.

5 Results and Discussion

EEG raw data acquisition was implemented using Python with emokit, as we used an Emotiv Epoch wireless headset with 14 electrodes discretized at 128Hz. The Fourier transform was written in real-time with NumPy. We computed the 4 areas $\times$ 6 frequency range EEG energy, then Python shared the 24 cerebral activity indicators by UDP at 10Hz.

More than 200 people experimented with the setup during the Siana exhibition [Catala 2015]. Before wearing the headset, users' hair was lightly sprayed with water. The Emotiv headset required some alterations and some welding repairs but our algorithmic choices proved robust: even if only 4 electrodes actually operate (one in each area), the whole set of indicators remains available. This was very important in the public context, with such a delicate sensor.

To connect the EEG to the sea waves, artists took the following values for 8 gravity wave group maps:

map	$\frac{2\pi}{k}$	dir.	$a \cdot k$	EEG activity indicator
1	125 m	SW	0.4	θ back left
2	115 m	WSW	0.5	θ back right
3	35 m	W	0.6	α front left
4	30 m	WNW	0.65	α front right
5	14 m	NW	0.8	β back left
6	12 m	NNW	0.85	β back right
7	3 m	N	0.9	β front left
8	2.5 m	NNE	0.95	β front right

where $2\pi/k$ is the wavelength, dir. the direction of wave propagation and $a \cdot k$ is the mean steepness at group centers. All instant phases were between $\pi/8$ for swell and $\pi/4$ for wind-sea waves. The group densities range from 4 for swell to 2 for short wind-sea waves.

From an oceanographic point of view, a sea state tells a story: offshore, a moderate wind was blowing from the south west six hours ago, then it slowly turned west two hours ago, and then veered north west twenty minutes ago, strengthening. Now it is blowing from north north east and it is stormy.

Drawing on a discretisation of Hinsinger et al. model [2002], the sea surface mesh of ten square kilometers is a home-made mesh with hexagonal symmetries and one million vertices; its triangle

[5] In contrast to wave groups in Belemaalem et al. that are λ-Poisson randomly distributed. This simplification facilitated GLSL model implementation.

[6] https://unity3d.com/

density decreases from its center to its edge in 4 steps: close, quite near, far, distant. It is used during flight to follow the 3D viewer with a succession of discrete steps with as few moving triangles as possible.

In the Unity3D per pixel shader, the 3 computed textures for the normal map correspond to:

NNE minus 5^o	30cm wavelength	low γ-EEG
NNE	11cm wavelength	medium γ-EEG
NNE plus 5^o	4cm wavelength	high γ-EEG

The 3D viewer is set at an altitude of two meters and in an easterly direction, towards the full moon which is at an elevation of 40 degrees. The moonlight is specular and gray in color, varying between black and white depending on the user's mood as calculted from the α-EEG at the front right and left of the scalp.

With the fastest rendering mode in Unity3D and a simple Intel Sandybridge Mobile graphic chipset, the animation runs at six Hertz in full screen mode [1366×768] (while the setup is running, the CPU is free for other computations). With the best rendering mode in Unity3D and a Geforce GTX 660, animation runs at 35Hz in full screen mode [1280×1024]; this increases to 55Hz if a good, rather than the best rendering mode is chosen.

The framed paragraph below is the $\approx$ 5-minute story of a user's experience from the point of view of a spectator:

> Noone is wearing the headset; the light is off and flight speed is null.
> Someone is wearing the headset. The light turns on in a few seconds and flight begins.
> The sea is flat and it is windy; in less than 10 seconds, short very choppy waves appear.
> Over the next 10 seconds, flight speed is constant (10m/s); the sea state becomes rougher and rougher.
> The scenario differs with different users. The moonlight oscillates from dark to bright. The sea state alternates between a smooth surface with high long waves and more choppy conditions with short waves and gusts. Some people try to turn left or right.
> And then the user removes the headset. Gusts immediately stop and the sea surface becomes oily. Short waves disappear in a few seconds. Then only the swell remains as the flight speed reduces and light slowly turns off after more than half a minute.
> The setup is ready for the next user to try, as illustrated by our movie [Thery et al. 2015].

The experience varies widely depending on whether one is a spectator or the user. Unlike the spectators, the users understand and experience their thoughts and fantasies while playing with the setup.

We would like to have more information about how users react to the setup, but the only available information was the one orally reported by technicians working on site. We need another context in which we can scientifically measure user perception.

6 Conclusion

As part of an art and science project, we have successfully connected EEG readings to a virtual sea scene. In this scene, the EEG controls flight direction, the moonlight colour is controlled by emotions and cerebral activity is converted in the form of wind action onto wave heights. We have described a non-linear choppy groupy wave model for animating ocean waves with group effects and strong horizontal asymmetries in real-time. The resulting setup was tested by two hundred users and we are encouraged by its reliability, which suggests it would be suitable for more widespread distribution.

Many hypotheses need to be scientifically explored from a human point of view; for example how could the users' perception of influence on the sea state be improved? or is the sea model able to generate a plausible sea state? Such a setup could also be used for original neurofeedback experiences.

Regarding the future of the choppy groupy wave model, we hope, for example, that it will allow artists to create overhanging effects which are not dissimilar to the actual physics of oceanography. Future works should explore its ability to simulate actual sea states, in terms of elevation, speed, slope and curvature fields over several square kilometers of ocean.

Acknowledgements

Lots of thanks to François Goujon, who created the audio part of this project; to Frédéric Devillers, engineer at the European Center for Virtual Reality (CERV), who introduced us to Unity3D with a beautiful Mastin-like sea animation; to Yoann Neveu-Dérotrie who completed his internship at CERV (summer 2014) and initiated us to Emokit; to Nathan Colin, Jeremy Crestel, Alban Delamarre, Nicolas Marsille (fall 2014) and Xiao Hang Wu, Yannick Guern, Simon Teneau (Autumn 2014) students at ENIB who experimented with the EEG connection to sea states.

References

BELEMAALEM, Z., CHAPRON, B., PARENTHOEN, M., AND REUL, N. 2010. The groupy-choppy wave model for simulating dynamical sea surface. In *OCOSS'2010 Proceedings*. 5p.

BIRBAUMER, N. 2006. Breaking the silence : Brain-computer interfaces (BCI) for communication and motor control. *Psychophysiology 43*, 6, 517–532.

BOS, D. P.-O., REUDERINK, B., LAAR, B., GÜRKÖK, H., MÜHL, C., POEL, M., NIJHOLT, A., AND HEYLEN, D. 2010. *Brain-Computer Interfaces*. Springer London, ch. Brain-computer interfacing and games, 149–178.

CATALA, L. 2015. Flavien Thery, Plastique de la lumiere et experiences sensorielles. *mcd, magazine des cultures digitales 11* (avril), 16–17.

CHATONSKY, G. 2013. *Dislocation VII : Suspension of attention*. http://chatonsky.net/projects/suspension-of-attention/.

DARLES, E., CRESPIN, B., GHAZANFARPOUR, D., AND GONZATO, J.-C. 2011. A survey of ocean simulation and rendering techniques in computer graphics. *Comput. Graph. Forum 30*, 1, 43–60.

DONELAN, M., AND DRENNAN, W. 1996. Nonstationary analysis of the directional properties of propagating waves. *Journal of Physical Oceanography 26*, 9, 1901–1914.

FATOURECHI, M., BASHASHATI, A., WARD, R. K., AND BIRCH, G. E. 2007. EMG and EOG artifacts in brain computer interface systems : A survey. *Clinical Neurophysiology 118*, 480–494.

FOURNIER, A., AND REEVES, W. 1986. A simple model of ocean wave. *Computer Graphics 13*, 75–84.

HINSINGER, D., NEYRET, F., AND CANI, M.-P. 2002. Interactive animation of ocean waves. In *Symposium on Computer Animation (SCA)*, 161–166.

JONES, N., AND FOX, N. 1992. Electroencephalogram asymmetry during emotionally evocative films and its relation to positive and negative affectivity. *Brain and Cognition 20*, 2, 280–299.

KOMEN, G., CAVALERI, L., DONELAN, M., HASSELMANN, K., HASSELMANN, S., AND JANSSEN, P. 1994. *Dynamics and modelling of ocean waves*. Cambridge University Press.

LÉCUYER, A., LOTTE, F., REILLY, R. B., LEEB, R., HIROSE, M., AND SLATER, M. 2008. Brain-computer interfaces, virtual reality, and videogames. *Computer 41*, 10, 66–72.

LIU, A., PENG, C., CHAPRON, B., AND MOLLO-CHRISTIENSEN, E. 1995. Direction and magnitude of wind stress over wave groups observed during SWADE. *Global Atmosphere and Ocean System 3*, 175–194.

MASTIN, G., WATTERGER, P., AND MAREDA, J. 1987. Fourier synthesis of ocean scenes. *Computer Graphics 14*, 16–23.

MEYERS, S., KELLY, B., AND O'BRIEN, J. 1993. An introduction to wavelet analysis in oceanography and meteorology: with application to the dispersion of Yanai waves. *Monthly Weather Review 121*, 10, 28–58.

MIN, L. 2013. *Project LIAison, EEG:EGG*. Life Sciences Institue, University of Michigan, http://www.project-liaison.org/#!eegegg/cii6.

NIELSEN, M. B., AND BRIDSON, R. 2011. Guide shapes for high resolution naturalistic liquid simulation. *ACM Trans. Graph. 30*, 4 (July), 83:1–83:8.

NIELSEN, M. B., SÖDERSTRÖM, A., AND BRIDSON, R. 2013. Synthesizing waves from animated height fields. *ACM Trans. Graph. 32*, 1 (Feb.), 2:1–2:9.

PARENTHOEN, M., JOURDAN, T., AND TISSEAU, J. 2004. IPAS: Interactive Phenomenological Animation of the Sea. In *International Offshore and Polar Engineering Conference (ISOPE)*, J. S. Chung, M. Prevosto, and H. S. Choi, Eds., vol. 3, International Society of Offshore and Polar Engineering, 125–132.

PARK, L. 2013. *Eunoia*. http://thelisapark.com/#/eunoia.

PEACHEY, D. 1986. Modeling waves and surf. *Computer Graphics 20*, 4, 65–74.

RENARD, Y., LOTTE, F., GIBERT, G., CONGEDO, M., MABY, E., DELANNOY, V., BERTRAND, O., AND LÉCUYER, A. 2010. Openvibe: An open-source software platform to design, test, and use brain–computer interfaces in real and virtual environments. *Presence: Teleoper. Virtual Environ. 19*, 1 (Feb.), 35–53.

STANSELL, P., WOLFRAM, J., AND ZACHARY, S. 2003. Horizontal asymmetry and steepness distributions for wind-driven ocean waves from severe storms. *Applied Ocean Research 25*, 137–155.

TESSENDORF, J. 2001. Simulating ocean water. In *SIGGRAPH, Courses Notes*, 3–1–3–18,45–62.

THERY, F., MURIE, F., PARENTHOEN, M., AND GOUJON, F. 2015. *La mer est ton miroir*. Siana, Speculaire, Lab-STICC, https://vimeo.com/124299171.

VIDAURRE, C., AND BLANKERTZ, B. 2010. Towards a cure for BCI illiteracy. *Brain Topography 23*, 2, 194–198.

ZAKHAROV, V. E. 1968. Stability of periodic waves of finite amplitude on the surface of a deep fluid. *Journal of Applied Mechanics and Technical Physics 9*, 2, 190–194.